
This is an electronic reprint of the original article.
This reprint may differ from the original in pagination and typographic detail.

Jussila, Vilho; Fülöp, Ludovic; Mäntyniemi, Päivi; Puttonen, Jari

A novel method of estimating earthquake durations for the analysis of floor vibrations of nuclear power plants

Published in:
Nuclear Engineering and Design

DOI:
[10.1016/j.nucengdes.2024.113606](https://doi.org/10.1016/j.nucengdes.2024.113606)

Published: 01/12/2024

Document Version
Publisher's PDF, also known as Version of record

Published under the following license:
CC BY

Please cite the original version:
Jussila, V., Fülöp, L., Mäntyniemi, P., & Puttonen, J. (2024). A novel method of estimating earthquake durations for the analysis of floor vibrations of nuclear power plants. *Nuclear Engineering and Design*, 429, Article 113606. <https://doi.org/10.1016/j.nucengdes.2024.113606>

This material is protected by copyright and other intellectual property rights, and duplication or sale of all or part of any of the repository collections is not permitted, except that material may be duplicated by you for your research use or educational purposes in electronic or print form. You must obtain permission for any other use. Electronic or print copies may not be offered, whether for sale or otherwise to anyone who is not an authorised user.



A novel method of estimating earthquake durations for the analysis of floor vibrations of nuclear power plants

Vilho Jussila^{a,*}, Ludovic Fülöp^b, Päivi Mäntyniemi^c, Jari Puttonen^a

^a Aalto University, Department of Civil Engineering, P.O. Box 12100, FI-00076 Aalto, Finland

^b VTT Technical Research Centre of Finland, P.O. Box 1000, FI-02044 VTT, Finland

^c Institute of Seismology, University of Helsinki, P.O. Box 68 (Pietari Kalmin katu 5), FI-00014 Helsinki, Finland

ARTICLE INFO

Keywords:

Arias intensity
Duration of ground-motion
Floor vibrations
Nuclear power plant

ABSTRACT

Many low-seismicity countries such as Finland have adopted IAEA requirements and recommendations for seismic design of new and existing nuclear power plants (NPPs). In low seismic regions, the structural seismic design is associated with floor vibration of NPPs. The floor vibration analysis is usually conducted in the time domain for which maximum amplitudes are retrieved from design spectra while the duration of ground motion is estimated as an interval between 5% and 75% of accumulation of the Arias intensity. As this method was developed for active seismic regions, it often overestimates the duration for the regions with low seismicity. The present article introduces a new twofold method for estimating the duration. First, the Arias intensity is calculated for a complete and consecutively reduced accelerograms resulting in a deviation curve. Second, this curve is simplified by a piecewise linear regression fitting. The simplified deviation curve has a linear time frame that includes the most significant part of the Arias intensity. The length of the time frame defines the effective duration of a specific ground motion. This implies that the effective duration depends directly on the ground motion instead of predefined percentiles of the Arias intensity. In this study, the method was applied to a set of ground accelerations adopted from eastern Canada, which is geologically similar to the Fennoscandian Shield where appropriate recordings are absent. The results showed that the durations depend on distance, but they were insensitive of magnitude for short rupture distances. This indicates that smaller events can also be useful for estimating the durations even though they do not meet the requirement of design basis earthquake in terms of the peak ground acceleration. The durations obtained with the proposed method were typically shorter than those based on the 5%–75% criterion. The durations received can be used to generate the acceleration time histories compliant with the design response spectra. We also propose durations with different rupture distances for the seismic design of the structures, systems, and components of nuclear facilities in Finland. In a feasibility study, we calculated floor vibrations of a generic reactor building using 3D finite element analysis. The results show that floor accelerations are very similar, when the base accelerogram is complete or shortened to the length proposed in this study.

1. Introduction

The International Atomic Energy Agency (IAEA) provides requirements and recommendations to ensure safety of nuclear power plants (NPPs) in safety standards. In many low-seismicity countries such as Finland, IAEA's seismic design standard (IAEA, 2021) has influenced to regulations for new NPPs and re-evaluation of existing NPPs. In Finland, the Radiation and Nuclear Safety Authority (STUK) defines provisions for external hazards for NPPs, including seismic events, that are the primary threats for nuclear safety (STUK, 2019). The provisions

define two conditions: the design basis earthquake (DBE) and the design extension conditions (DEC). All nuclear utilities shall prove that these design events do not cause catastrophic failures of structures, systems and components (STUK, 2019). In regions of low seismicity, the faults contributing to the seismic hazard are usually unknown leading to use of probabilistic seismic hazard analysis (PSHA, McGuire, 2008), based on areal source zones. PSHA provides uniform hazard spectra (UHS) with given annual frequencies of exceedance for the site of interest. Design spectra is obtained by smoothening the UHS. The design spectra provide acceleration amplitude for DBE or DEC. However, duration must be

* Corresponding author.

E-mail address: vilho.jussila@aalto.fi (V. Jussila).

<https://doi.org/10.1016/j.nucengdes.2024.113606>

Received 29 May 2024; Received in revised form 28 August 2024; Accepted 18 September 2024

Available online 26 September 2024

0029-5493/© 2024 The Authors. Published by Elsevier B.V. This is an open access article under the CC BY license (<http://creativecommons.org/licenses/by/4.0/>).

defined separately to transform the design spectra to time domain. A typical solution for the problem is to adopt the duration from ASCE 4-98 (2000, 2017) or NRC (2020) as done by Jussila et al. (2016) and Dundulis (2017). The duration estimates by ASCE (2017) and NRC (2020) are based on predefined integral limits of energy and Arias intensity (1970) respectively. These limits are suitable for seismically active regions, but the limits may result in overestimated duration for regions of low seismicity, and on very-hard rock (VHR) sites. ASCE (2000) applied by Jussila et al. (2016) and Dundulis (2017) did not provide a relationship between the duration and the distance. Rupture distances¹ (Abrahamson and Silva, 1997) 50–80 km from magnitude range of M_w 4–6 contribute most to seismic hazard for NPPs in Finland (Fülöp et al., 2023). In addition, all NPP sites are on VHR, with shear wave velocity more than 3000 m/s. This indicates that a realistic value for the dominating duration is obviously shorter than 10 s, which was used by Jussila et al. (2016) and Dundulis (2017). At the regions of low seismicity, the response of NPP structures to DBE usually remains within elastic range. Therefore, the main concern is the evaluation of the seismic capacity of different systems and components, which requires the calculation of linear floor response spectra at multiple locations in the NPP. The target of this research is to define durations needed for calculating these floor response spectra.

In regions of low seismicity, a common practice is that parameters for seismic design are adopted from the regulations developed for seismogenic areas. The practice has been extended to ground motions, e.g. ground-motion prediction equation (GMPE) or PSHA. An example of adopting the parameter is the evaluation of the floor vibration calculations by Jussila et al. (2016) and Dundulis et al. (2017), who used American Society of Civil Engineers (ASCE) 4-98 (2000), a regulation developed in the USA for analyzing a hypothetical reactor building in Finland and the Ignalina NPP in Lithuania, respectively. The lack of relevant ground-motion records in Finland calls for the retrieval of seismic data from similar geological conditions elsewhere, typically Eastern North America and eastern Canada, complemented with Western Australia. Many GMPE and PSHA studies for NPP sites in Finland have relied partly or completely on ground motions from eastern Canada (Varpasuo et al., 1999; Sandberg et al., 2008; Fülöp et al., 2020; Fülöp et al., 2023). Similarly, in the 1980 s and earlier, seismic designs in eastern Canada relied on ground motions from California, due to insufficiency of observations (Weichert, 1985). Indications that ground motions from eastern Canada are suitable for Finland are available in the study by Fülöp et al. (2020). They developed a GMPE for Fennoscandia, showing that at similar rupture distances, PGAs up to M_w 4.2 in Fennoscandia overlapped well with the PGAs used in the development of the Next Generation Attenuation Relationships for Central & Eastern North America (NGA-East) GMPE (Goulet et al., 2021).

The duration is primarily dependent on the magnitude and rupture distance. The problem is to isolate the period from the ground-motion data that contributes most to the structural damage. Defining the arrivals of body waves is straightforward. However, determining the moment when the body waves have passed the observation location can be indistinct. The reason is that the arrivals of scattered seismic waves mask direct body waves. The methods used to isolate the most damaging period for structures can be divided into three groups: bracketed and uniform duration, significant duration, and structural methods. These methods were mainly developed to estimate the strong motion duration of large earthquakes (Bommer and Martínez-Pereira, 1999), which are producing highly non-linear structural responses. Both bracketed and uniform durations use thresholds of accelerations to limit the parts of the acceleration recording considered as strong motion. With bracketed

durations, strong motion is the total time between the first and last peaks in the accelerogram exceeding the threshold, while in uniform durations the strong motion is the sum over time of the values exceeding the threshold. Acceleration thresholds proposed for bracketed and uniform durations include 0.03 g by Ambraseys and Sarma (1967), 0.05 g by Page et al. (1972), and Bolt (1973). The significant duration methods are those based on the cumulative integral of the acceleration history, while the duration of strong motion is defined as the time difference of a predefined interval of accumulation of the intensity. More recently, Taflampas et al. (2009) proposed a new definition for the duration of strong motion by combining bracketed and significant durations. The structural method proposed by Zahrah and Hall (1984) uses single-degree-of-freedom (SDOF) linear oscillators and the criterion of effective motion, which is defined as a development of dissipation energy (E_d) over time. The main sources of dissipation are damping and inelastic yielding. The energy boundaries were 5 %, 75 %, and 90 % of the total energy dissipated, while the effective duration is defined as the time used between the 5 % and 75 % levels of energy dissipation. Below 5 % and above 90 %, it was argued that the main source of dissipation is damping. Xie and Zhang (1988) used SDOF oscillators and the concept of yielding acceleration. In their method, the strong motion duration is directly associated with the yield strength of the structure. Applying bracketed and uniform durations or structural methods in a region of low seismicity, where moderate earthquakes and suitable ground-motion recordings are sparse, may lead to a structural design that is overly unconservative and unjustified.

A classical approach to calculate the significant duration of strong motion is usage of the Arias intensity (I_A) (Arias, 1970). However, the intensity was originally developed to define earthquake destructiveness by a simple method that is independent of the dynamics of the structure and has as few parameters as possible. Arias assumed a degree of proportionality between structural damage and the energy dissipated by the structure. The I_A is defined as the integral of structural dissipation or linear strain energy per unit weight. The I_A was used for the first time to estimate strong motion duration, when Husid (1969) plotted the cumulative integral of the I_A as a function of time. Later, Trifunac and Brady (1975) defined the 5 %–95 % limits for the accumulation of the I_A , which covers most of the ground motions. The limits can be chosen such that they cover the linear part of the accumulation. The United States Nuclear Regulatory Commission NRC (2020) and ASCE 4-16 (2017) incorporates the idea in their definition of the 5 %–75 % accumulation of the I_A and energy, respectively. Furthermore, in analysis of the collapse capacities of a five-story building, Chandramohan et al. (2016) applied 5 %–75 % and 5 %–95 % accumulation of the I_A . The application of the I_A has not been limited to structural analysis. In the development of the prediction equations for significant durations as a function of M_w , Kempton and Stewart (2006) applied the 5 %–75 % accumulation of the I_A . Since the 5 %–75 % and 5 %–95 % accumulations of the I_A could be applied from micro to major earthquakes, Bommer and Martínez-Pereira (1999) defined the effective duration as a time interval between the I_A ordinates from 0.01 m/s to 0.125 m/s. Furthermore, if the I_A remains below 0.135 m/s, the record is disregarded. Applying effective duration by Bommer and Martínez-Pereira (1999) to NPPs in Finland may lead to limited numbers of ground-motion records. On the other hand, the 5 %–75 % accumulation of the I_A tends to result in overconservative durations for moderately-sized earthquakes, since the 5 %–75 % accumulation of the I_A should cover the linear range. However, in our analysis the 5 %–75 % accumulation frequently extended to the nonlinear section, resulting in over-conservative durations.

The objective of this study is twofold. The first objective is to provide a method to estimate the duration of small to moderate earthquakes for calculating the floor vibrations of the NPP in seismically quietest regions. The second objective is to show that the method is applicable for various rupture distances and several moment magnitudes. We propose durations of earthquakes for NPPs in Finland. These durations were calculated by using proxy events from eastern Canada, because M_w of

¹ We use rupture distance concept to retain equivalence with related publications i.e. Fülöp et al. (2020); Jussila et al. (2021) and Fülöp et al. (2023). Rupture distance is approximately equal with hypocenter distance for small and moderate earthquakes (Fülöp et al., 2020).

the available recordings in Finland from short rupture distances are not enough large and the bedrock is approximately similar to Finland in terms of shear wave velocity. The magnitudes included in the duration estimation were M_w 3.5–5.9, the largest event of which was the Saguenay earthquake of 25 November 1988 (Munro and North, 1988). This article is divided into six sections. Section 2 describes the new method, and Section 3 provides general notes on implementation and selected events. Section 4 shows the obtained ranges for the durations, while in Section 5 we show feasibility of the proposed method by analyzing floor vibrations of a reactor building. In Section 6, we discuss the implications of the results. Finally, in Section 7, we discuss the conclusions.

2. A new method for calculating ground motion duration

In considering ground-motion history, the first wave observed is the pressure or P-wave, which is followed by the shear or S-wave. The ground-motion history also includes surface and coda waves, which are reflected and scattered waves that follow the direct waves. The coda waves are present in the later part of the recordings and mask portions of the S-waves. The characteristics of these various wave types are dependent on factors such as the magnitude, rupture distance, subsurface geology, and even the acquisition and processing techniques used. In general, the amplitudes of P-waves are smaller than those of S-waves, surface waves, and coda waves (Kramer, 1996). Thus, P-waves play lesser roles in contributing to the strong motion recorded on the ground surface. The arrivals of S-waves and surface waves are indicated by a sudden increase in ground-motion amplitude. Within short rupture distances, coda waves (Aki and Chouet, 1975) are less distinctive, but at longer rupture distances they play significant roles in estimating the duration of ground motions applied to structural analyses.

The new method is based on the deviation of the I_A (Arias, 1970) between complete and repeatedly reduced time frames of ground motions. The I_A of ground motions as applied to the calculation of duration is dependent on the energy stored in an SDOF spring mass system, which is excited by the acceleration time histories of the ground motions $\ddot{x}_{ground}(t)$. The displacements $x(t)$, velocities $\dot{x}(t)$, and accelerations $\ddot{x}(t)$ of the oscillating mass are received as a solution of the constant-coefficient linear-second-order differential equation

$$\ddot{x}(t) + 2\xi\omega_n\dot{x}(t) + \omega_n^2x(t) = -\ddot{x}_{ground}(t) \quad (1)$$

where ω_n is the natural frequency of the spring mass system in rad/s and ξ is the constant damping ratio over a range of natural frequencies. Integrating Equation (1) with respect to displacement dx or $\dot{x}dt$ results in kinetic energy, E_d , and linear strain energy. If $x(0) = x(\infty) = \dot{x}(0) = \dot{x}(\infty) = 0$, then the kinetic energy and the linear strain energy vanish. However, as the SDOF oscillator consumes the kinetic energy of the ground-motion by the E_d , it leads to an equation

$$E_d = 2\xi\omega_n \int_0^\infty \dot{x}^2(t)dt = - \int_0^\infty \ddot{x}_{ground}(t)\dot{x}(t)dt \quad (2)$$

Arias²⁸ defined the intensity I of ground motions as an integral of the E_d of the SDOF oscillator per unit weight in the frequency domain

$$I = \frac{1}{g} \int_0^\infty E_d(\omega)d\omega \quad (3)$$

where ω is the angular frequency. Inserting Equation (2) into Equation (3) gives the I_A an expression

$$I_A(\xi) = \frac{\cos^{-1}(\xi)}{g\sqrt{1-\xi^2}} \int_{t_0}^{t_1} \ddot{x}_{ground}^2(t)dt \quad (4)$$

where the integral limits t_0 and t_1 indicate the beginning and end of the ground-motion time frame, respectively. When the damping ratio is $\xi = 0$, Equation (4) approaches a limiting value of

$$I_A(0) = \frac{\pi}{2g} \int_{t_0}^{t_1} \ddot{x}_{ground}^2(t)dt \quad (5)$$

ASCE 4-16 (2017) uses the concept of cumulative energy, which differs from Equation (5) by the constant factor of $\pi/(2g)$. Both quantities are equivalent in the proposed method, providing the same results. However, in the presentation here, we use Arias intensity. The proposed new method begins with selection of a complete time frame indicated by a rectangle with the solid line in Fig. 1. The left edge of the complete time frame should contain the arrival of the P-wave, if available, while the simplest selection for the right edge is at the end of the ground-motion data. Selection of the complete time frame follows the calculation of the I_A of it. In this calculation, we assumed that the damping ratio is zero and the I_A of the complete acceleration time frame I_c equals to the Arias intensity $I_A(0)$ when the boundaries of the integration are zero and infinity. In the next step, the length of the complete time frame is decreased by a time increment Δt , resulting in a reduced time frame indicated by a rectangle with a dashed line in Fig. 1. Calculation of the Arias intensity I_s of the reduced time frame leads to relative deviation d of I_s and I_c , which is evaluated as

$$d = \frac{I_s - I_c}{I_c} 100 \quad (6)$$

The computation process is repeated until $d \approx 100\%$ (Fig. 2). The time dependency of the deviation curve is created by tracking the location of the left edge of the time frame, as illustrated in Fig. 1.

The accelerogram of earthquake ground motions follows a certain pattern. The amplitudes recorded by a modern seismogram contain noise from the environment before the arrival of the P-wave. If the left edge of the complete and reduced time frame includes noise in the intensity calculation, then the outcome of Equation (6) is nearly 0 % deviation. Similarly, if the acceleration amplitudes are small between the arrivals of the P-waves and S-waves, compared with the S-wave acceleration amplitudes, the deviation is close to 0 %. Otherwise, within this section, the deviation may gently slope. Once the reduction in the time frame reaches the arrival of the S-wave, the deviation increases suddenly. This point indicates the moment when the relevant ground motions are not included in the time frame or when the relevant duration of the ground motion begins. Two patterns may be identified when the time frame is further reduced. In the first case, the deviation attains a value of $\sim 100\%$ in a short time, creating a deviation curve with two or three distinct kinks, as illustrated in Fig. 2 (a). In this case the end point for the duration is distinctive and clear, and the described behavior is typical for recordings at short rupture distances. In the second case, the deviation increases gradually, but visual conclusion of the end point can be subjective, since the deviation curve approaches the time axis progressively, as shown in Fig. 2 (b). This is typically associated with recordings at longer rupture distances, which have distinctive decay envelopes in the acceleration amplitudes. To avoid subjective decisions in determination of the end point for the duration, the deviation curve is approximated with a piecewise-linear regression fitting. The main requirement for this fit is that the locations of abrupt gradient changes between linear segments, known as break-points, are defined with a quantitative method. A suitable method was the piecewise-linear regression fitting by Muggeo (2003), which fits the linear line models and break-points iteratively to the intensity deviation curve. The main feature of the proposed method is that the steepest linear part of the deviation curve between two break-points contains the strongest ground motion in the accelerogram. Usually, the steepest section is between the first and second break-points. Therefore, the time difference between the first and second break-points is the duration recommended for use in generating acceleration histories for structural analyses.

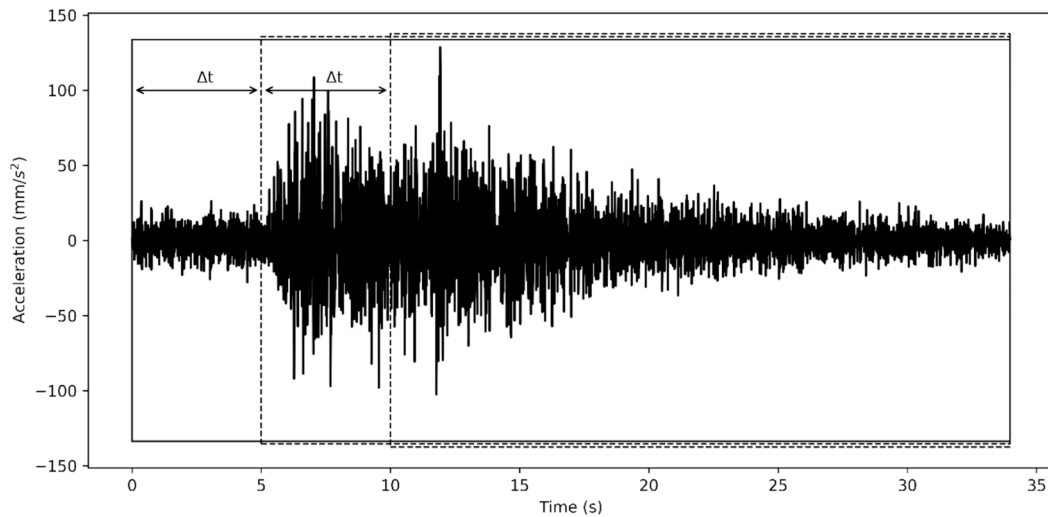


Fig. 1. Illustration of the reduction in the time window by Δt . The rectangle with the solid line indicates the complete time frame and the rectangles with the dashed lines represent reduced time frames.

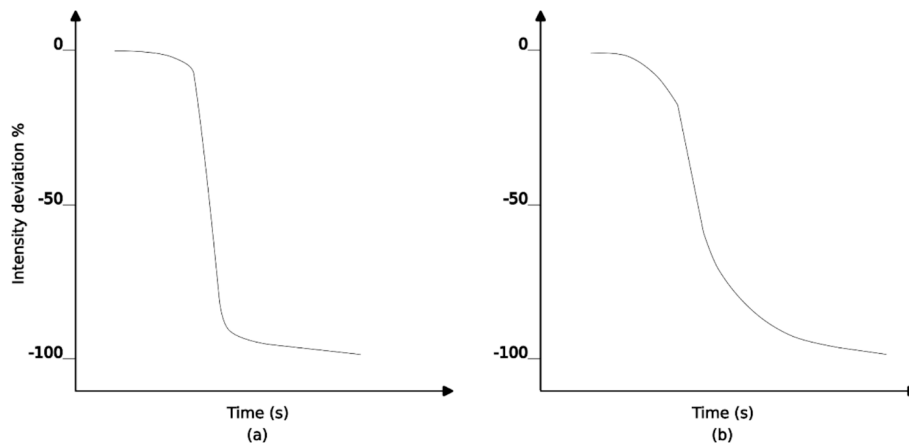


Fig. 2. Schematic plot of the deviation curve when the rupture distance is short (a) and long (b).

3. Implementation of the proposed method

The proposed method was implemented with Python, utilizing publicly available SciPy (Virtanen et al., 2020), NumPy (Harris et al., 2020) and piecewise-regression (Pilgrim, 2021) site-packages. These tools provide powerful methods for calculating ground-motion duration. However, the events selected, the number of break-points applied to the piecewise linear regression fitting, and the selection of a representative duration for three axial accelerometers require closer scrutiny, all of which are covered in the following subsections.

3.1. Earthquake events

The International Federation of Digital Seismograph Networks (FDSN) has stored waveform data from the Canadian National Seismograph Network since 1992 (Natural Resources Canada, 1975). An alternative resource is The Engineering Seismology Toolbox (Assatourians and Atkinson, 2010). Neither of these web services includes any information on the strongest event recorded in the region, the Saguenay earthquake of 25 November 1988 (Munro and North, 1988; Somerville et al., 1990), which was M_s 6.0 on the surface wave magnitude scale. The waveforms of the Saguenay 1988 earthquake were directly requested from Natural Resources Canada, the remaining events were downloaded from The Engineering Seismology Toolbox

(Assatourians and Atkinson, 2010). From this web service the selected events were $m_N \geq 4.0$ on the Nuttli magnitude scale (Nuttli, 1973), which is empirically associated with moment magnitudes M_w (Sonley and Atkinson, 2005), namely

$$M_w = 1.03m_N - 0.61 \quad (7)$$

A total of 22 events were available for determination of the earthquake duration (Table 1). For events $4.0 \leq m_N < 5.0$ on the Nuttli scale, the selected stations were no further than rupture distances up to 100 km. However, for events $m_N \geq 5.0$, the selected stations were at rupture distances up to 300 km, as were the data used for the Fennoscandia GMPE (Fülop et al., 2020). Selection of the stations was not exclusively controlled by the distance. The foundation of a station site should be on hard rock since that serves as the foundation for NPPs in Finland. Therefore, the seismic stations located on soil were excluded. The study by Ladak et al. (2021) led to the assumption that most of the stations were founded on hard rock. Moreover, their study confirmed that several station foundations indeed are on hard rock, while only a single station foundation was on soft rock. The seismic stations recording the Saguenay waveforms were mainly bolted on limestone bedrock (Munro and North, 1988).

Table 1

Selected events (Natural Resources Canada, 1975, Assatourians and Atkinson, 2010) for estimating duration of ground motions, M_s = surface-wave magnitude, M_w = moment magnitude, m_N = Nuttli magnitude.

Event number	Date	Magnitude m_N	Magnitude M_s	Magnitude M_w	Epicenter latitude	Epicenter longitude	Depth (km)
1	1988/25/11	–	6.0	5.9	48.121°N	71.186°W	28
2	1992/11/17	4.4	–	3.9	45.770°N	74.930°W	16
3	1994/09/25	4.3	–	3.8	47.770°N	69.960°W	17
4	1996/03/14	4.4	–	3.9	45.920°N	74.400°W	18
5	1997/10/28	4.7	–	4.2	47.670°N	69.910°W	11.3
6	1997/11/06	5.1	–	4.6	46.800°N	71.420°W	22.5
7	1998/04/18	4.1	–	3.6	45.580°N	74.970°W	18
8	1998/07/30	4.4	–	3.9	46.190°N	74.800°W	10
9	1999/10/31	4.2	–	3.7	45.860°N	74.300°W	18
10	2000/01/01	5.2	–	4.7	46.840°N	78.930°W	12
11	2000/07/12	4.2	–	3.7	47.560°N	71.060°W	18
12	2002/01/20	4.1	–	3.6	49.490°N	66.950°W	30
13	2002/04/20	5.5	–	5.1	44.530°N	73.730°W	18
14	2002/07/23	4.0	–	3.5	49.590°N	66.950°W	18
15	2003/06/13	4.1	–	3.6	47.700°N	70.090°W	11.1
16	2005/03/06	5.4	–	5.0	47.750°N	69.730°W	13.3
17	2005/10/20	4.3	–	3.8	44.680°N	80.480°W	11
18	2006/01/09	4.2	–	3.7	45.030°N	73.900°W	15
19	2006/02/25	4.5	–	4.0	45.650°N	75.230°W	20
20	2006/04/07	4.1	–	3.6	47.380°N	70.460°W	24.5
21	2006/12/07	4.2	–	3.7	49.510°N	81.530°W	16
22	2008/11/15	4.2	–	3.7	47.740°N	69.740°W	13.3

3.2. Time step Δt

The repetitive reduction of the complete time frame by the constant time step Δt implies down-sampling of the ground-motion data. A time step Δt that is equivalent to sampling of the ground-motion data results in a less smooth, but more accurate deviation curve. However, Fig. 3 shows that a 1.0-s time step predicts the onset of the gradient change well, while a 3.0-s time step predicts the too early beginning of the gradient change. The 1.0-s time step does not necessarily result in a feasible approximation, as subplot (b) in Fig. 3 shows that a time step of 1.0 s predicts onset of the gradient change well while a time step of 3.0 s predicts the too early beginning of the gradient change. The time step of 1.0 s does not necessarily result in feasible approximation as the subplot (b) in Fig. 3 shows. In this case, the time step should be 0.5 s instead of 1.0 s, because the rupture distances of ground motion in subplots (a) and

(b) of Fig. 3 are 69.7 km and 14.6 km respectively. The 1.0-s time step is simply too long for the ground motions at short rupture distances. Therefore, the time step chosen for rupture distances ≤ 50 km was 0.5 s, while for longer distances the time step was 1.0 s.

3.3. Break-points for fitting piecewise linear regression to the intensity deviation curve

Approximating the intensity deviation curve with a piecewise-linear regression fitting requires definition of the number of break-points. Python implementation (Pilgrim, 2021) of the piecewise-linear regression fitting by Muggeo (2003) does not have an upper bound for the number of break-points, but the target is to avoid overfitting. On the other hand, it is impossible to find a single value for the number of break-points that applies to all the events in Table 1. Thus, the number of

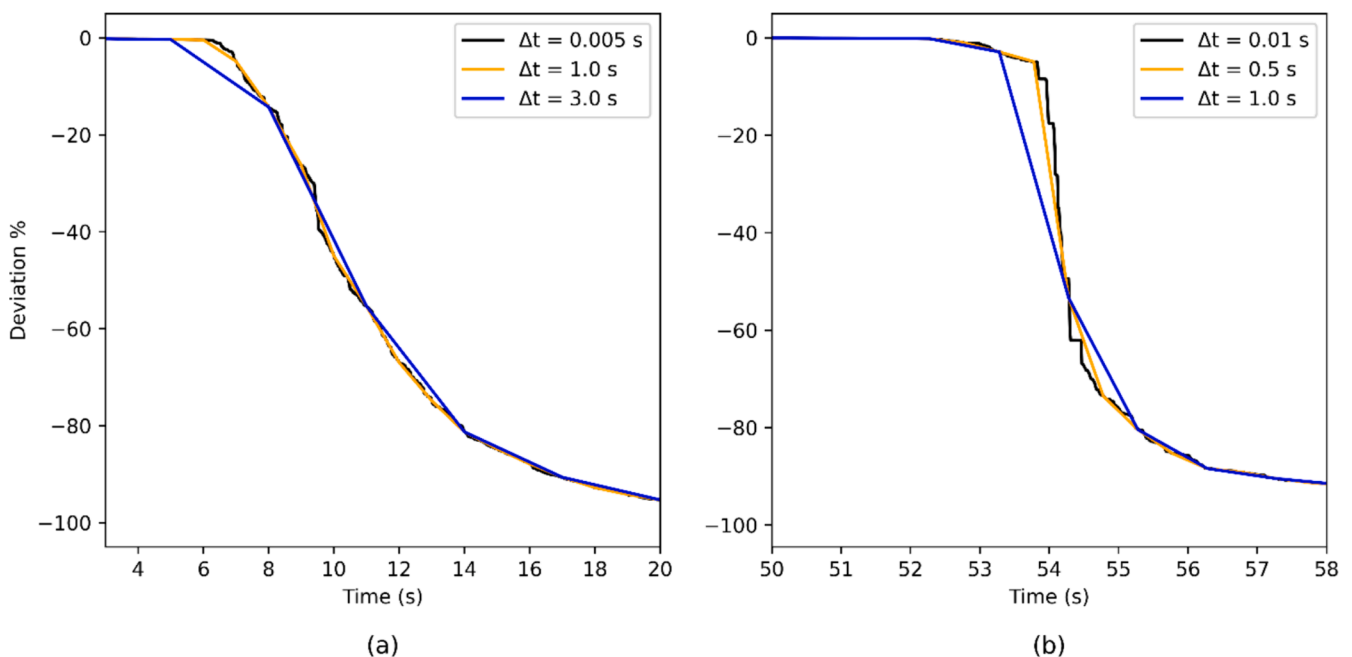


Fig. 3. Deviation curves for varying time step Δt . In subplots (a) and (b), the rupture distances are 69.7 km and 14.6 km, respectively.

break-points is specific for each accelerogram, but generally two or three break-points are enough to fit piecewise-linear lines into the deviation curve. Since the algorithm for finding break-points is iterative, a quantitative measure is needed to assess the locations of the break-points on the time axis. A suitable measure is the confidence intervals, which are based on the t-distribution with a standard error of 5 %. A narrow confidence interval indicates that the position of the break-point is stable, while a wide interval indicates that the position is sensitive to the iteration process. As an example, piecewise linear regression fitting with three break-points and their 95 % confidence intervals are illustrated in subplot (b) of Fig. 4, while subplot (a) shows the duration estimate defined by the time interval between the first and second break-points. Since the first and second break-points define the duration, the 95 % confidence intervals of their locations are important, while the third, as shown in Fig. 4 (b), is less relevant for the duration, but required for fitting a piecewise-linear regression into the intensity deviation curve.

3.4. Duration of triaxial seismogram

A modern seismogram is typically triaxial, resulting in three values for the duration and intensity of ground motions. The acceleration components differ in frequency content and amplitudes, resulting in variation among the durations and intensities evaluated for each component. The representative duration at each station in Table 1 can either be defined by the longest duration or the largest intensity of three components. Moderate or small earthquakes recorded with a triaxial seismogram at longer rupture distances may have a component with clearly smaller amplitudes or longer acceleration time histories, compared with other components. This may artificially result in over-estimation of the duration, as demonstrated in Table 2. These durations were calculated as the 5 %–75 % accumulations of the I_A given in Equation (5). The HHZ component has the longest duration of about 16.1 s, while the HHN has the greatest intensity for which the calculated duration is about 8.1 s. In comparing the differences in duration and intensity between components HHZ and HHN, HHN has clearly shown that while its duration is about 7.4 s shorter than that of HHZ, it also has about three times greater intensity than HHZ. Thus, the assumption is that the component having the greatest intensity, regardless of its duration, is the one most capable of damaging structures. Therefore, the representative duration for each station in Table 1 was defined based on the I_A of the accelerograms.

4. Results

Earthquake records from eastern Canada were applied to the estimates of ground-motion durations calculated with the proposed method for structural analyses of NPPs situated in seismically quiescent regions. The analyses of 71 earthquake records resulted in durations that were defined by the time differences between the confidence intervals of the break-points of piecewise linear regressions fitted in the deviation curves. To compare the results of the proposed method with those of the existing method, reference durations were calculated with the 5 % and 75 % accumulations of I_A . This is referred to in the subsequent sections as the reference method. The results of the 95 % confidence intervals are followed by the results that show similarities and differences between the proposed method and the reference method. The rest of this section focuses on the main results, which are the durations as a function of rupture distances.

4.1. Results of 71 earthquake records

The results of 71 earthquake records consist of record numbers, event numbers, M_w , rupture distances, PGAs, and durations. These durations were calculated with the 5 % and 75 % accumulations of the I_A , using the break-points of the deviation curves, and are shown in Table 3. The event number refers to Table 1, while the first five columns in Table 3 describe the events. The PGA values can be used to evaluate these events regarding the threshold values of bracketed and uniform durations. Since the analyzed accelerograms represent moderate earthquakes, the PGA values calculated from the ground-motion data vary from 0.001 g to 0.217 g. Comparing the PGAs in Table 3 to the threshold value of 0.03 g by Ambraseys and Sarma (1967) and 0.05 g by Page et al. (1972) and Bolt (1973) for the uniform duration and bracketed durations, indicates that 14 PGAs exceeded 0.03 g and 11 exceeded 0.05 g. However, record number 9 in Table 3 has a PGA value of 0.217 g and I_A over 350 mm/s (Fig. 5), which are greater than the PGAs and I_A of the record numbers 1–7, representing the largest considered event. This PGA and I_A is inconsistent compared to similar events in terms of the rupture distance and M_w . In considering the I_A as a function of rupture distance, Fig. 5 shows that 3 of 71 records exceeded the accelerogram acceptance value for the calculation of effective duration by (Bommer and Martínez-Pereira, 1999). Furthermore, the I_A suddenly increased at a rupture distance of ~ 50 km, which was caused by the Saguenay event in 1988 (Munro and North, 1988; Somerville et al., 1990). The durations

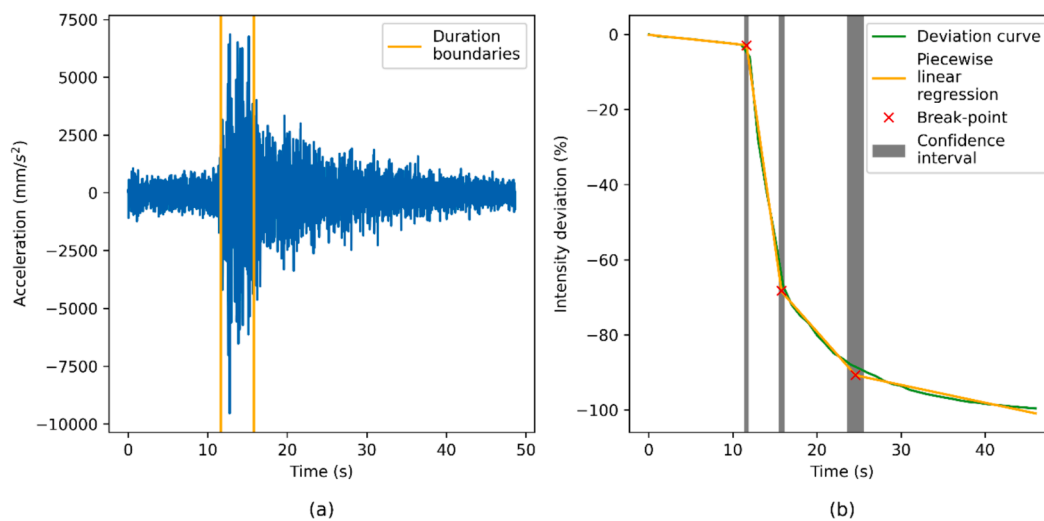


Fig. 4. Saguenay M_s 6.0 earthquake on 25 November 1988. In subplot (a) is the accelerogram from St-Ferreal Station, at a rupture distance of 117 km. Subplot (b) shows the intensity deviation curve in green, the piecewise regression fitting with three break-points indicated with the red crosses, and the 95 % confidence intervals in light blue bars. The orange vertical lines in subplot (a) indicate the first and second break-points in subplot (b). M_s = surface-wave magnitude.

Table 2

Example of an event with significant differences in intensity and duration among its components. M_w = moment magnitude.

Date	Magnitude (M_w)	Station	Component	Rupture distance (km)	Arias 5 %-75 % duration (s)	Arias intensity (mm/s)
2006/04/07	3.6	A21	HHE	72	8.65	1.22E-02
			HHN	72	8.71	1.49E-02
			HHZ	72	16.14	5.12E-03

calculated with the proposed method were based on the mean values of the 95 % confidence intervals of the break-points marking the boundaries of the linear section in the deviation curve. The mean duration and confidence intervals of the break-points are given in Table 3. Break-point 1 and break-point 2 indicate, respectively, the beginning (Fig. 6a) and end (Fig. 6b) of the linear section of each deviation curve. Both subplots show a clear increasing trend between the confidence intervals and the mean durations. However, of the linear section of each deviation curve. Both subplots clearly showed a tendency to increase between the confidence intervals and the mean durations. However, Fig. 6 shows that the increase in the 95 % confidence interval is independent of the M_w . If the duration is short, the 95 % confidence intervals are clustered, while with long durations the spreading of the 95 % confidence intervals is more prominent.

The proposed method applies the deviation curves of I_A in the mean duration estimates. These durations were compared with those calculated with the 5 %-75 % accumulations of the I_A to associate the proposed method with the reference method currently used. The ground-motion durations calculated with both methods are shown in Table 3. Generally, the durations calculated with the proposed method are shorter than those received, using the reference method. For instance, several stations at rupture distances less than 100 km have accelerograms in which the duration of significant amplitudes is short. These short durations may not be observed by the reference method, but may be captured by the proposed method, leading to significant differences in the estimated durations. Record 61 in Table 3 and subplots (a), (b) and (c) in Fig. 7 illustrates the situation. In this case, the rupture distance is 29 km, and the duration estimates with the proposed method and reference method are 1.4 s and 8.1 s, respectively. The methods resulted in a wide difference in duration for accelerogram 61 since the linear regression fitting can recognize a linear interval in the deviation curve of the I_A . In contrast, the 5 %-75 % intensity accumulation extended to the nonlinear interval of the intensity. The 8.1-s duration calculated with the reference method was inconsistent with the expectation of the ground-motion duration recorded at short rupture distances. Subplot (a) also shows that the duration of the acceleration-amplitude plateau was short, and the amplitudes decayed exponentially, justifying the short linear interval in subplots (b) and (c). Table 3 also includes cases, e.g. record 55, in which the duration estimates were similar. In this case, the rupture distance is 34 km, and both methods resulted in an estimated duration of 10.3 s. In Fig. 8, subplots (b) and (c) show that both methods remained in the linear range. This was caused by a relatively long duration of the acceleration-amplitude plateau in subplot (a), and within this plateau the I_A accumulated from 5 % to 75 % linearly. The proposed method does not consistently result in estimates of shorter durations, as illustrated with the results of record 3 in Fig. 9. In this case, the rupture distance is 95 km, and the duration with the proposed method and reference method is 10.7 s and 8.7 s, respectively. Similarly, as in record 55, the 5 %-75 % accumulations of I_A were approximately linear. However, subplot (b) shows that the fitting with two break-points resulted in slightly longer durations since the deviation curve tends to bend towards the time axis earlier than that estimated by the piecewise linear regression fitting, which can be a program-specific numeric feature.

4.2. Duration estimates by the reference method and the proposed method

The durations calculated with the reference and proposed methods in

Table 3 are given for each seismic station separately in subplots (a) and (b) of Fig. 10. These subplots show that the duration tends to grow steeply upwards at intermediate rupture distances between 50 km and 100 km, after which the growth rates tend to decrease. Fitting piecewise linear regression (Muggeo, 2003; Pilgrim, 2021) to all records in Table 3 results in reasonable description of this change. Fig. 10 shows that durations are widespread relative to the fitting indicated with the orange lines. Analysis of M_w distribution in subplots (a) and (b) of Fig. 10 shows that magnitudes from M_w 3.5 to M_w 4.0 and from M_w 4.0 to M_w 5.0 are quite evenly distributed but are also responsible for the largest exceedance of the fitted curve in both subplots. In contrast, magnitudes from M_w 5.0 to M_w 6.0 have durations, except for one below the fitted curve in subplot (a), while in subplot (b) three durations exceed the fitted curve. Comparison of subplots (a) and (b) in Fig. 10 show that the durations calculated with the reference method vary more widely than the mean durations calculated with the proposed method, which is also visible in the duration residuals shown in subplots (c) and (d). These results show that the proposed method reduces the durations independently of the rupture distance, and the variation is less scattered. In all, the duration residuals in subplots (c) and (d) of Fig. 10 are quite evenly distributed around the mean. This trend prevails up to a rupture distance of 170 km. At further distances, the duration residuals are close to the mean, but that range contains only four duration values.

In Table 4, the durations are given for rupture distances from 20 km to 100 km. These distances include the rupture distance range of the main seismic hazard for NPPs in Finland. For these distances, the calculated mean duration with the proposed method varies from 2.0 s to 7.3 s, while estimates for durations calculated with the reference method are from 4.1 s to 12.2 s. These values show that the duration estimates with the proposed method are about half as short as those in the reference method. The duration residual standard deviations were calculated for both methods, using the rupture distance ranges. The step size was 20 km, and the durations were for the upper limit of each rupture distance range d_r , except for the 50-km rupture distance. At this distance, the durations are in the middle of the range d_r . The proposed method and the reference method resulted in duration residual standard deviations from 0.8 s to 4.1 s and from 3.1 s to 7.4 s, respectively. However, in the proposed method the residual standard deviation decreased slightly at the 100-km rupture distance. Subplot (b) in Fig. 10 shows that the proposed method resulted in shorter mean durations over a range of 80–100 km than a range of 60–80 km, which explains the decrease in residual standard deviation. However, similar trends could not be observed in the durations of the reference method in subplot (a) of Fig. 10.

5. Feasibility study of the proposed duration

To demonstrate the influence of the proposed durations on floor vibrations, the analysis of a hypothetical NPP building was carried out following the study of Jussila et al. (2016). The floor vibrations were calculated with ABAQUS (ABAQUS, 2016) using modal dynamics, with natural frequencies up to 50 Hz and the corresponding mode shapes of the reactor building. The boundary conditions were base accelerations. In contrast with Jussila et al. (2016), who used Rayleigh damping, in this feasibility study the damping was 2 % over the natural frequency domain.

In floor vibration analysis, artificial accelerograms are typically applied to the base of the building. These accelerograms are the result of

Table 3

The event number refers to Table 1. Selected events were $M_w \geq 3.5$ and the longest rupture distance was 100 km and 300 km for events $M_w < 4.5$ and $M_w \geq 4.5$ respectively. All stations were on hard rock. Duration of the ground motion for selected events and stations. Durations calculated as time differences of the break-points on the deviation curve are the mean values of the confidence intervals. Break-point 1 and break-point 2 indicate 95 % confidence intervals for the mean at the beginning and end of the linear interval in the deviation curve. M_w = moment magnitude, PGA=peak-ground acceleration.

Record number	Event number	Station	M_w	Rupture distance (km)	PGA (g)	Duration (s) reference method	Duration (s) proposed method	Confidence intervals Break-point 1	Confidence intervals Break-point 2
1	1	St-Ferreol	5.9	117	0.121	7.4	3.9	±0.3	±0.4
2	1	Riviere-Ouelle	5.9	118	0.057	3.5	1.4	±0.1	±0.1
3	1	Chicoutimi-Nord	5.9	51	0.131	8.7	10.7	±1.2	±1.0
4	1	St-Andre	5.9	70	0.156	6.0	5.7	±0.4	±0.7
5	1	Quebec	5.9	152	0.051	3.4	2.5	±0.1	±0.2
6	1	La Malbaie	5.9	97	0.124	4.3	1.4	±0.1	±0.2
7	1	St-Pascal	5.9	126	0.056	10.7	4.8	±0.7	±0.7
8	2	GAC	3.9	46	0.066	4.1	1.4	±0.1	±0.2
9	3	LMQ	3.8	41	0.217	1.5	1.0	±0.1	±0.1
10	4	GAC	3.9	89	0.001	5.9	6.7	±0.3	±0.3
11	5	A11	4.2	53	0.001	14.2	3.8	±0.5	±0.5
12	5	A16	4.2	26	0.018	2.6	1.2	±0.1	±0.1
13	5	A21	4.2	20	0.027	3.6	3.4	±0.2	±0.2
14	5	A54	4.2	46	0.002	17.2	7.8	±0.5	±0.6
15	5	A61	4.2	18	0.059	0.3	0.9	±0.0	±0.0
16	5	A64	4.2	21	0.029	1.0	1.4	±0.3	±0.2
17	6	A11	4.6	107	0.002	13.7	5.9	±0.6	±0.7
18	6	A16	4.6	132	0.002	23.0	6.2	±0.8	±0.9
19	6	A21	4.6	166	0.006	20.8	14.3	±0.9	±1.4
20	6	A61	4.6	143	0.003	18.5	9.2	±0.9	±1.4
21	6	A64	4.6	164	0.002	21.4	15.9	±0.9	±1.4
22	7	GAC	3.6	46	0.001	7.8	1.4	±0.3	±0.2
23	8	GAC	3.9	76	0.001	9.2	6.0	±0.6	±0.8
24	9	GAC	3.7	95	0.000	6.0	7.7	±0.3	±0.4
25	10	SADO	4.7	231	0.001	10.1	7.0	±0.5	±0.5
26	11	A54	3.7	53	0.001	18.0	7.9	±1.0	±1.3
27	11	A61	3.7	76	0.002	18.9	9.6	±0.9	±1.2
28	11	A64	3.7	94	0.001	13.9	8.8	±0.7	±1.0
29	11	LMQ	3.7	58	0.002	12.9	10.4	±0.6	±0.7
30	12	ICQ	3.6	38	0.003	5.5	4.4	±0.2	±0.3
31	13	GAC	5.1	190	0.001	13.6	9.1	±0.6	±0.7
32	13	KGNO	5.1	223	0.002	12.0	7.9	±0.5	±0.6
33	13	MNT	5.1	110	0.002	13.1	10.5	±0.6	±0.8
34	14	ICQ	3.5	30	0.001	10.6	7.9	±0.5	±0.7
35	15	A11	3.6	53	0.000	18.8	13.5	±0.9	±1.2
36	15	A16	3.6	29	0.007	9.5	3.9	±0.9	±0.8
37	15	A21	3.6	32	0.003	10.7	0.9	±0.1	±0.1
38	15	A54	3.6	38	0.002	16.0	12.0	±0.5	±0.7
39	15	A61	3.6	11	0.029	0.7	0.9	±0.1	±0.1
40	15	A64	3.6	23	0.012	12.5	5.5	±0.5	±0.7
41	15	LMQ	3.6	27	0.004	13.6	1.2	±0.1	±0.2
42	16	A11	5.0	68	0.008	5.2	2.5	±0.2	±0.3
43	16	A16	5.0	40	0.031	3.3	0.8	±0.1	±0.1
44	16	A21	5.0	15	0.071	1.1	0.8	±0.1	±0.1
45	16	A54	5.0	62	0.016	7.8	3.1	±0.5	±0.5
46	16	A61	5.0	31	0.065	0.6	0.8	±0.0	±0.0
47	16	A64	5.0	20	0.035	6.7	1.8	±0.1	±0.2
48	16	ICQ	5.0	268	0.001	16.4	9.9	±0.6	±0.6
49	16	LMQ	5.0	52	0.026	7.8	2.1	±0.3	±0.4
50	17	BRCO	3.8	91	0.002	20.5	11.8	±1.1	±1.2
51	17	CLWO	3.8	31	0.008	16.8	9.4	±0.6	±0.8
52	17	KLBO	3.8	79	0.001	19.4	12.9	±1.0	±1.2
53	18	MNT	3.7	59	0.001	10.3	4.6	±0.6	±0.7
54	18	MRHQ	3.7	100	0.000	14.6	10.3	±0.6	±0.9
55	19	ALFO	4.0	34	0.007	10.3	10.3	±0.4	±0.5
56	19	GAC	4.0	28	0.015	0.5	0.6	±0.0	±0.0
57	19	OTT	4.0	51	0.004	6.6	3.7	±0.4	±0.6
58	20	A11	3.6	35	0.002	3.7	1.7	±0.1	±0.1
59	20	A16	3.6	43	0.010	5.3	1.0	±0.1	±0.1
60	20	A21	3.6	72	0.002	8.7	2.2	±0.2	±0.2
61	20	A54	3.6	26	0.009	8.1	1.4	±0.2	±0.2
62	20	A61	3.6	51	0.002	15.2	10.9	±1.0	±1.5
63	20	A64	3.6	70	0.002	13.6	13.1	±0.5	±0.7
64	20	LMQ	3.6	32	0.014	1.4	1.0	±0.1	±0.1
65	21	KAPO	3.7	73	0.001	7.9	4.8	±0.5	±0.7
66	21	OTRO	3.7	77	0.002	16.9	13.4	±0.7	±1.0
67	22	A16	3.7	38	0.002	12.6	11.0	±0.6	±0.7
68	22	A21	3.7	14	0.072	0.1	0.9	±0.0	±0.0

(continued on next page)

Table 3 (continued)

Record number	Event number	Station	M_w	Rupture distance (km)	PGA (g)	Duration (s) reference method	Duration (s) proposed method	Confidence intervals Break-point 1	Confidence intervals Break-point 2
69	22	A54	3.7	61	0.002	10.8	3.1	± 0.5	± 0.6
70	22	A64	3.7	20	0.019	1.1	0.6	± 0.1	± 0.1
71	22	LMQ	3.7	51	0.002	12.2	2.2	± 0.5	± 0.4

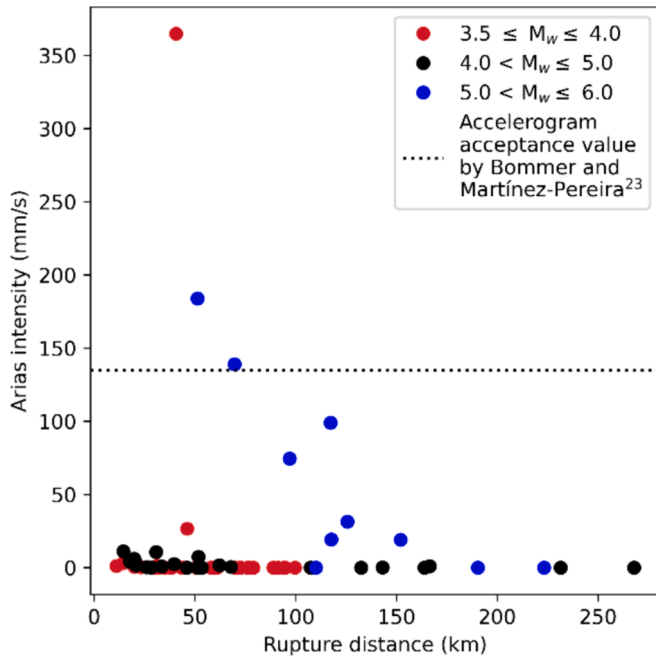


Fig. 5. The Arias intensity (Arias, 1970) as a function of the rupture distance. M_w = moment magnitude.

transformation of uniform hazard spectra to time domain. The duration of strong motion plateau of the transformation is usually considered equal between all three translational directions X, Y and Z. However, in the feasibility study it is more convenient to use natural accelerograms; in this case the challenge is that each translational component has different duration, as shown in Table 2, and equal duration needs to be proposed. It is also important that the durations with the reference method and the proposed method are significantly different, to demonstrate the duration effects. Accelerograms from St-Ferreol station

(Table 3) fulfill this criterion because the durations are 3.9 s and 7.4 s by the proposed and reference method. To show the feasibility of the proposed method the floor vibrations were calculated using accelerograms with three different durations: (i) the completed accelerogram, (ii) the plateau of strong motion by the reference and (iii) the proposed method. Since the plateau of strong motion cannot begin and end instantaneously, we extend these durations by the linear rise time of 1.2 s and the linear decay time of 4.0 s. Fig. 11 shows the accelerograms in the three directions. Following these considerations of the base accelerograms, the floor vibrations presented by Jussila et al. (2016) were re-analyzed.

The grid of output nodes has an influence on the floor vibration statistics (Jussila et al. 2016). This study adopted the 2 m grid, and the nodes selected by the engineering judgement from Jussila et al. (2016). The acceleration time histories were calculated from the 4th floor, as well as single nodes from the 4th and 6th floor. These node sets are indicated with red dots in Fig. 12. Pseudo-spectral acceleration (PSA) and cumulative distribution function (CDF) for the peak-floor acceleration were calculated and compared for floor accelerations induced by the full and the shortened base-accelerograms.

The results of the feasibility study for single nodes on the 4th (Fig. 13) and 6th (Fig. 14) floors show that PSAs are very similar in the Y and Z directions, while in the X direction small differences are present. Fig. 15 shows CDFs of peak acceleration ordinates of PSAs for the 4th floor. The CDF values from 0.2 to 0.8 in the X direction have some deviation in the floor accelerations induced by the full, reference and proposed accelerograms. The deviation is not exclusively present in the CDF of the PSAs of the proposed method, but also clearly visible in the CDF of the PSAs of the reference method. However, in the X direction the CDFs from 0.8 to 1.0 show very similar accelerations.

6. Discussion

The methods currently used to estimate the durations of ground motions for structural analysis of NPPs include the significant duration, bracketed and uniform duration, and structural methods. The threshold values of 0.03 g and 0.05 g proposed for the bracketed and uniform

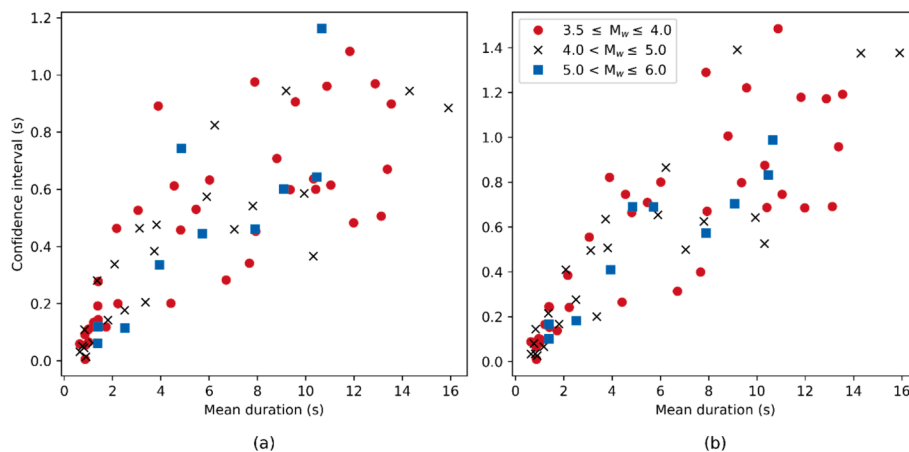


Fig. 6. Subplots (a) and (b) show the 95 % confidence intervals of the break-points as a function of the durations at the beginning and end of the significant interval. The break-points in subplots (a) and (b) represent the moments when the linear sections of the deviation curves begin and end. M_w = moment magnitude.

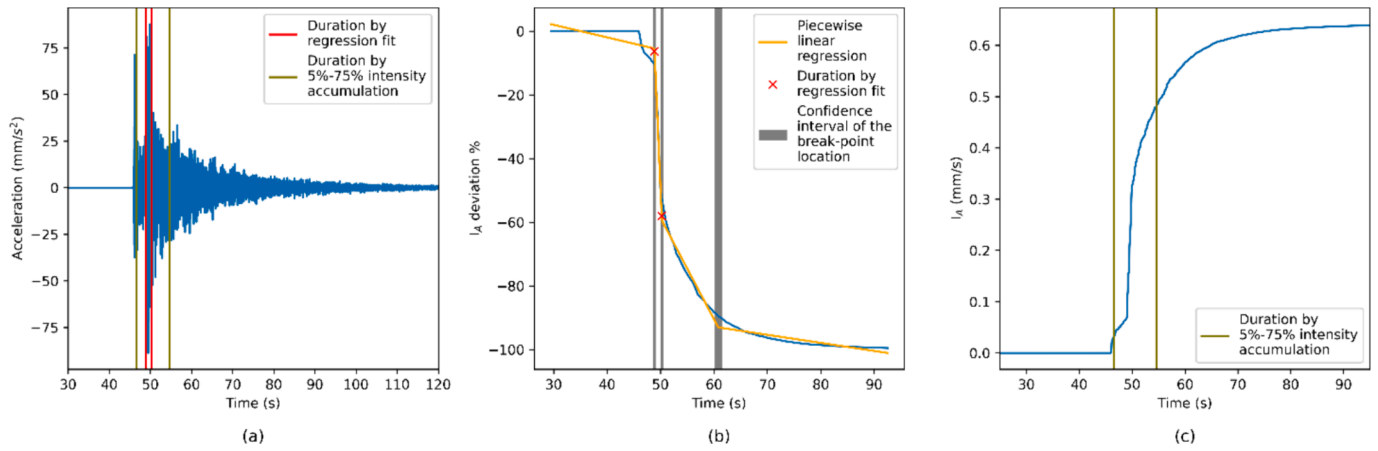


Fig. 7. Subplot (a) shows the acceleration time history of record 61 in Table 3. The vertical red lines in subplot (a) define the duration in which the time difference between the break-points is indicated with red crosses in subplot (b). The vertical olive lines in subplots (a) and (c) represent the interval between the 5% and 75% accumulations of the Arias intensity (I_A). The duration in subplot (b) is 1.4 s, which is shorter than the 8.1-s estimate in subplot (c).

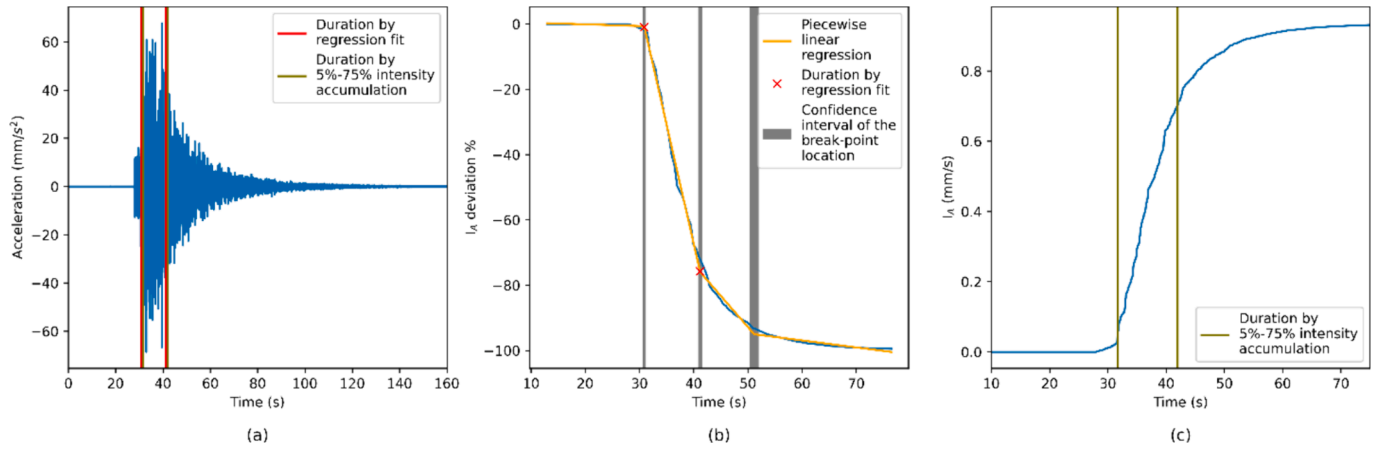


Fig. 8. Subplot (a) shows the acceleration time history of record 55 in Table 3. The vertical red lines in subplot (a) define the duration in which the time difference between the break-points is indicated with red crosses in subplot (b). The vertical olive lines in subplots (a) and (c) represent the interval between the 5% and 75% accumulations of the Arias intensity (I_A). Subplots (b) and (c) show equal duration estimates of 10.3 s.

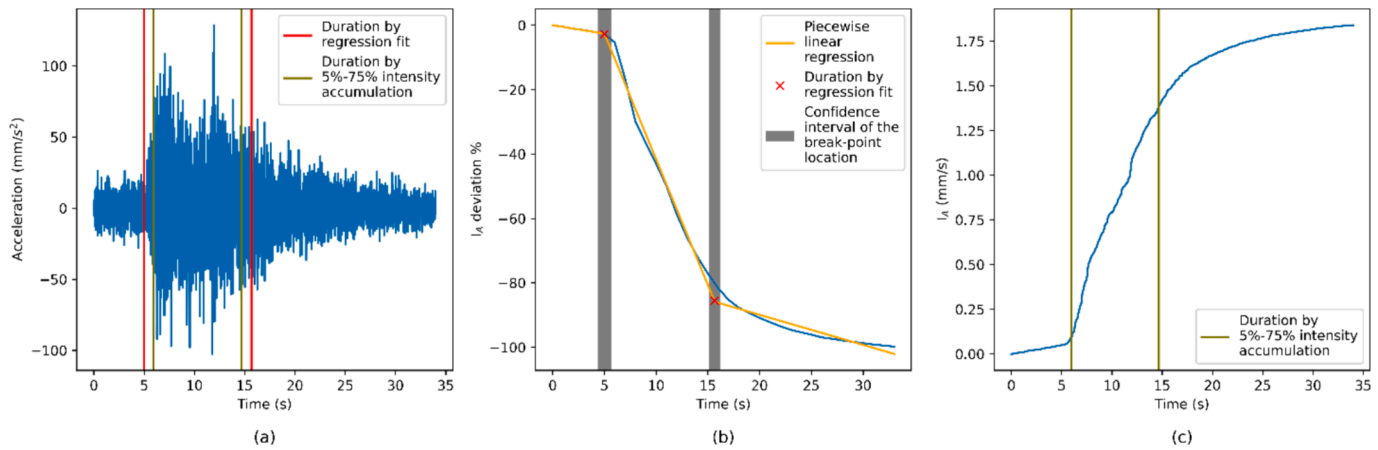


Fig. 9. Subplot (a) shows the acceleration time history of record 3 in Table 3. The vertical red lines in subplot (a) define the duration in which the time difference between the break-points is indicated with red crosses in subplot (b). The vertical olive lines in subplots (a) and (c) represent the interval between the 5% and 75% accumulations of the Arias intensity (I_A). The duration in subplot (b) is 10.7 s, which is longer than the 8.7-s estimate in subplot (c).

duration methods have reduced their suitability for the structural analysis of NPPs in low-seismicity regions such as Finland. Limited numbers of ground motions from earthquakes in SCRs recorded at very

hard rock sites approach these threshold values (Ambraseys and Sarma, 1967; Page et al., 1972; Bolt, 1973). As Table 3 shows, only 14 and 11 PGA values exceeded the thresholds of 0.03 g and 0.05 g, respectively.

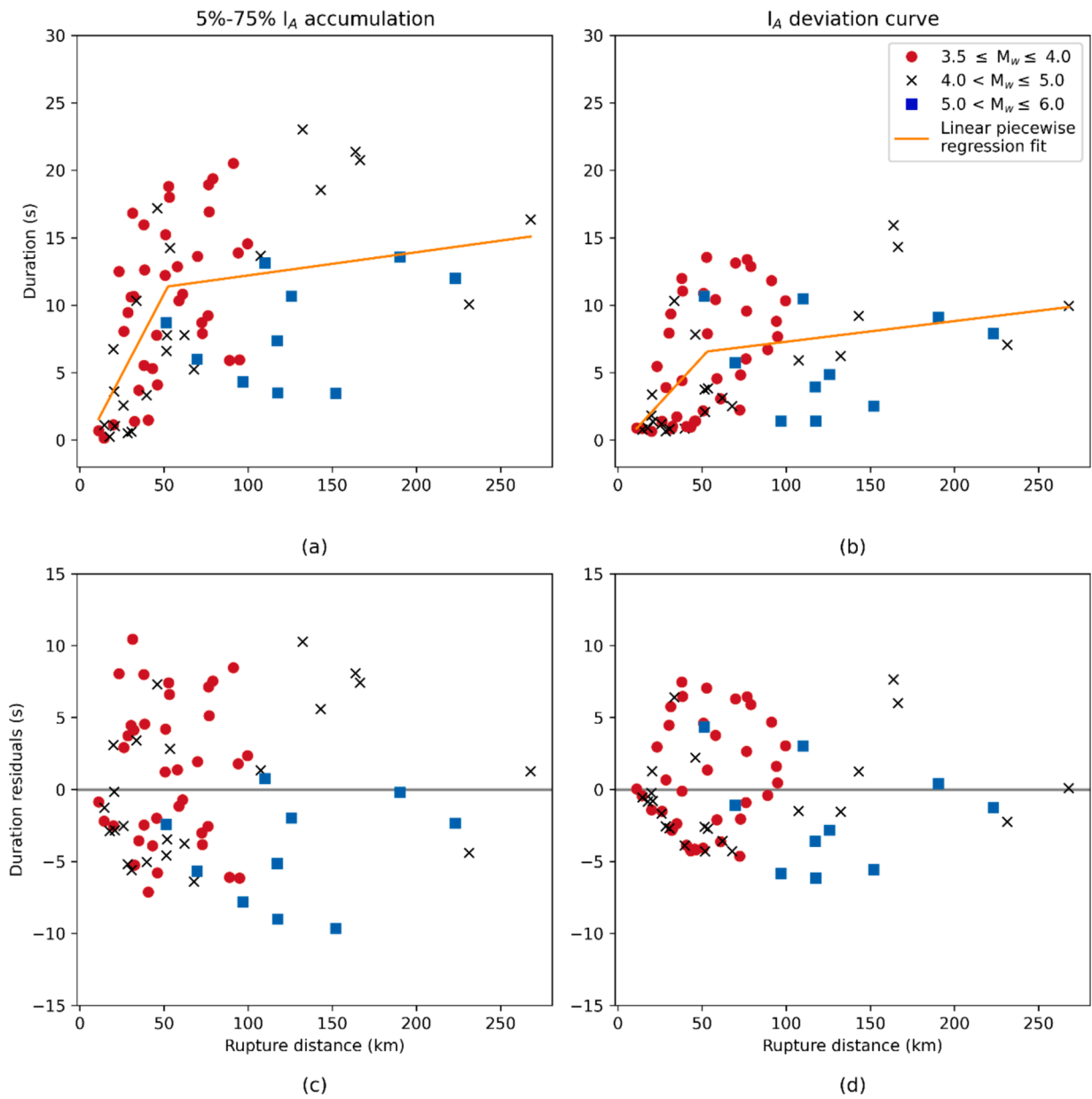


Fig. 10. Subplots (a) and (b) show the duration as a function of the rupture distance. Subplot (a) contains the durations calculated from the 5%–75% accumulations of the Arias intensity (I_A). Subplot (b) contains the durations based on the deviation curves. Subplots (c) and (d) describe the duration residuals.

Table 4

Duration estimates for several rupture distances obtained by proposed method. I_A = Arias intensity.

Rupture distance (km) for the mean duration	Rupture distance range d_r (km) for the duration residual standard deviation	Duration by 5%–75% accumulation of I_A (s)	Mean duration by piecewise linear fit to I_A deviation curve (s)
20	$0 < d_r \leq 20$	4.1 ± 3.1	2.0 ± 0.8
40	$20 < d_r \leq 40$	8.5 ± 5.6	4.7 ± 3.9
50	$40 < d_r \leq 60$	10.7 ± 5.0	6.1 ± 4.2
60	$40 < d_r \leq 60$	11.5 ± 5.0	6.7 ± 4.2
80	$60 < d_r \leq 80$	11.9 ± 5.3	7.0 ± 4.7
100	$80 < d_r \leq 100$	12.2 ± 7.4	7.3 ± 4.1

On the other hand, using the bracketed and uniform duration methods may lead to severe underestimation of the duration, since typically only a limited number of cycles have exceeded the threshold value. The

effective duration method defined by Bommer and Martínez-Pereira (1999) has an accelerogram acceptance threshold value of 0.135 m/s, which reduces ground-motion records from 71 to 3. This is simply too few records for estimating the duration for structural analysis of NPPs and argues against the use of the method. Applying structural methods may lead to an underestimation of the duration, since NPP structures are not expected to be damaged by earthquakes in regions of low seismicity. To estimate the duration of earthquake ground motions for NPPs, current practice relies on accumulation of the I_A . However, as discussed by Bommer and Martínez-Pereira (1999) accumulation between the 5% and 75% of I_A should not be applied to all ground acceleration records. This was confirmed by our results here, as shown in Fig. 7 and in Table 4. For instance, the longest duration in Table 4 (20.5 s) was retrieved, using the reference method for the site at rupture distances less than 100 km. The main reason for such a long estimate for duration is that the 5%–75% threshold included nonlinear parts of the accumulation curve of I_A , as shown by the example in Fig. 7. This result contrasts with the requirement that the accumulation curve of I_A should remain in the linear range

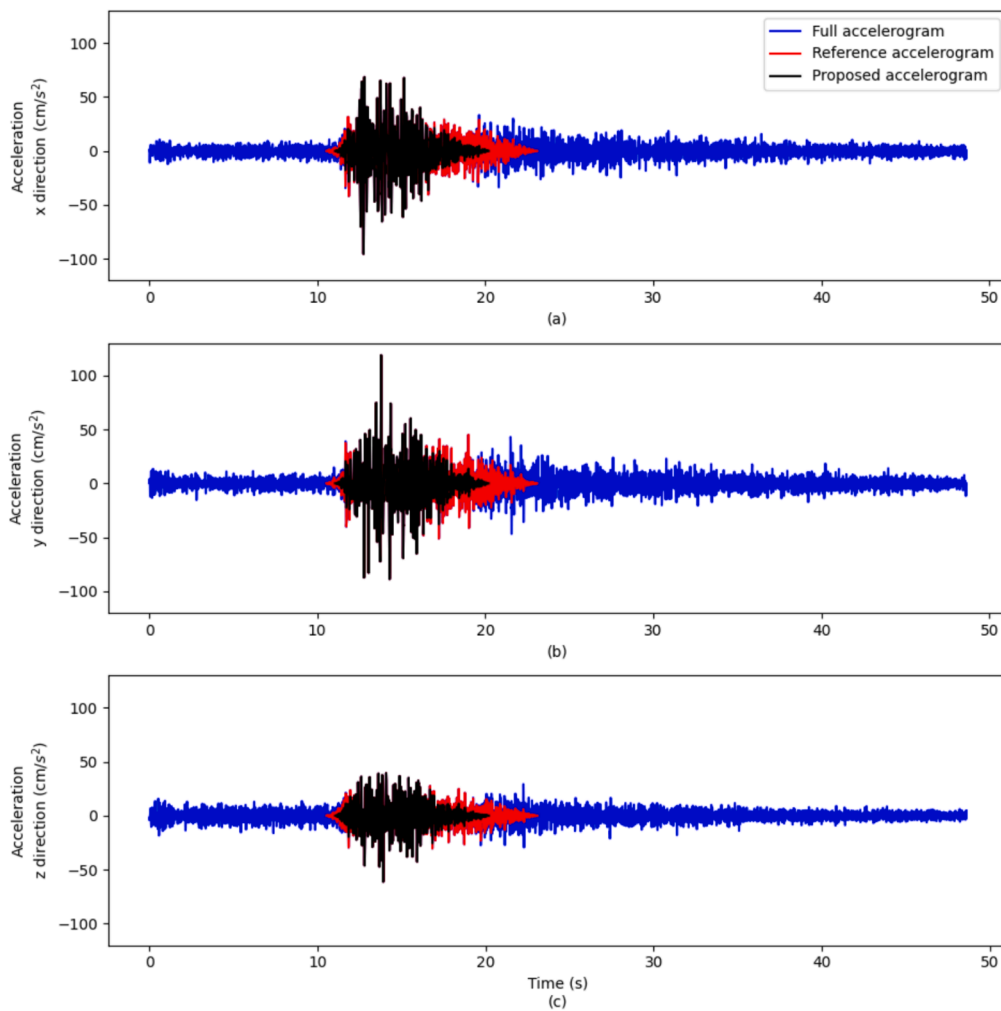


Fig. 11. Accelerograms of the Saguenay earthquake 1988 recorded at the station St-Ferreeol. The duration of the full acceleration recording is 48.6 s (blue line). The durations by the reference method are 7.4 s (red line), while the method proposed in this paper proposes a duration of 3.9 s (black line). The reduced duration accelerograms include the 1.2 s rise time and 4 s decay time respectively.

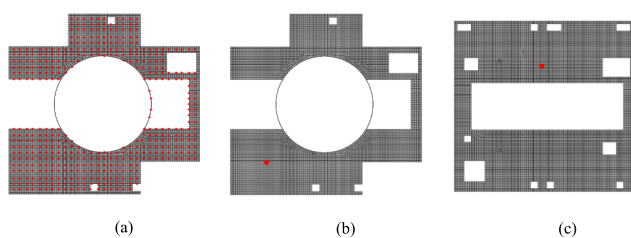


Fig. 12. Analyzed nodes are highlighted in red. In subplots (a) and (b) describe the 4th floor. The first one is the 2 m grid and the second is a single node from the engineering node set. In subplot (c) is a single node from engineering node set from the 6th floor. A detailed description of these node sets is given by Jussila et al. (2016).

(NRC, 2020). As Table 3 and Fig. 10 show, the durations retrieved with the proposed method are mainly shorter than those calculated with the accumulation curve of I_A . In some cases, both methods result in similar durations, as shown in Fig. 8. The common factor in these cases is that both methods remain in the linear range. This generally indicates that longer duration estimates with the reference method compared with the proposed method are the result of including the nonlinear part in the accumulation curves of I_A . The duration estimates should be driven by features in the ground-motion data instead of predefined limits. These

results emphasize that the 5%–75% accumulation of I_A is not a suitable method for SCRs, that may occasionally have moderate earthquakes.

Due to the limited number of suitable seismic events for structural design of NPPs in Finland, several decisions were made regarding magnitude, rupture distance, and piecewise linear regression fitting. The magnitudes of the selected events were $3.5 \leq M_w \leq 6.0$ to obtain reasonable data coverage for the duration estimations. However, low PGA values in Table 3 indicate that these events are only feasible to define duration. Transformation of design response spectra to accelerogram corrects amplitudes to meet the requirements in regulations. Based on the piecewise linear regression plots and residual plots in Fig. 10, expanding the minimum M_w to 3.5 may somewhat extend the durations at the rupture distances below 100 km, but a very-hard rock environment dominated by elastic wave propagation, the durations received by the method are evenly distributed regardless the M_w . This indicates that smaller events can also be useful for estimating the durations even though they do not meet DBE or DEC levels in terms of PGA. As Fig. 6 demonstrates, the increase in mean duration widens the confidence intervals. This implies reduced distinguishability of the beginning and end of the linear range in the deviation curves. The reason for the reduced distinguishability is the influence of scattered seismic waves, which mask direct body waves. The masked ground motions become more prominent in the distant recordings of smaller magnitude events, while considering that the main seismic hazard is in the range of 50–80 km for NPPs in Finland. These reasons led to the upper limit of

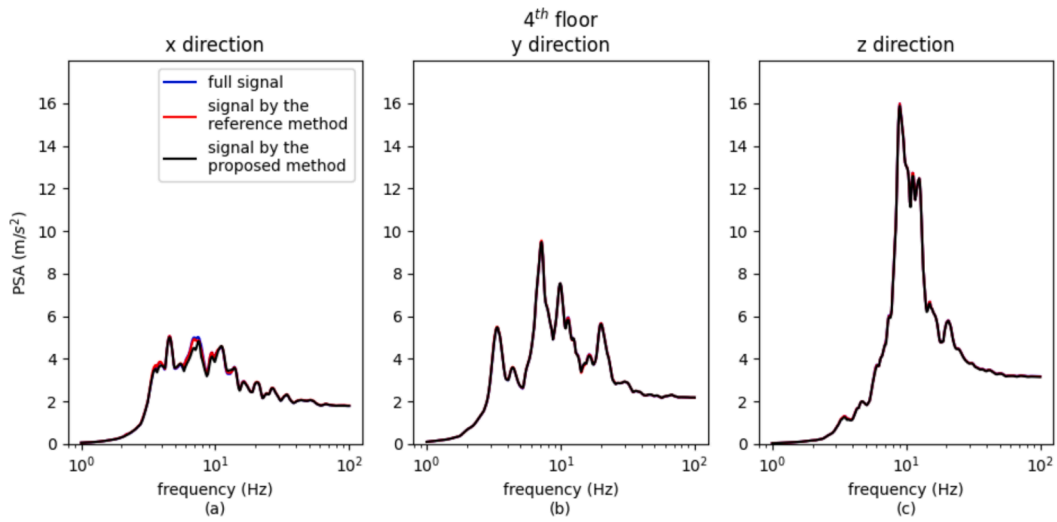


Fig. 13. PSAs calculated for the node in subplot (b) of Fig. 12 by using accelerograms in Fig. 11. PSAs of full, reference and proposed accelerograms are in blue, red and black.

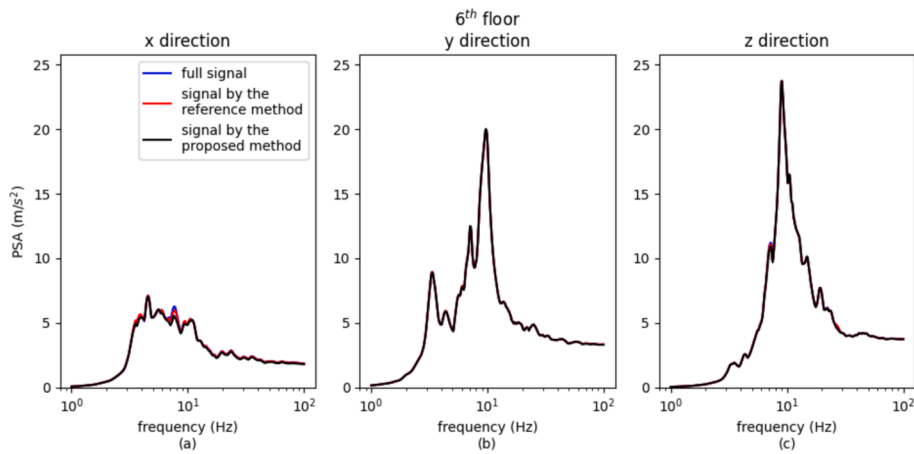


Fig. 14. PSAs calculated for the node in subplot (c) of Fig. 12 by using accelerograms in Fig. 11. PSAs of full, reference and proposed accelerograms are in blue, red and black.

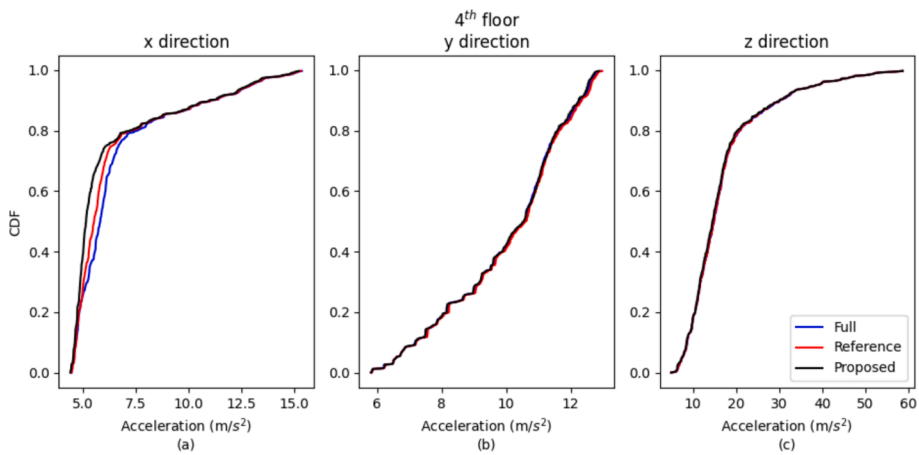


Fig. 15. CDFs of peak accelerations ordinates of PSAs for the 2 m grid of 4th floor. Blue, red and black indicate CDFs of peak accelerations ordinates of PSAs calculated from floor vibrations excited by the full, reference and proposed accelerograms.

100 km for the rupture distance when the M_w were $3.5 \leq M_w \leq 4.5$. The piecewise linear regression fitting was applied to all the seismic records in Table 3 instead of grouping the records into magnitude bins. The reason for this decision was that otherwise a very limited number of events would control the duration estimates of each bin. For instance, a bin for $5.0 < M_w \leq 6.0$ would include two events, as Table 1 shows. On the other hand, using all the records to estimate the ground-motion durations may hide detailed information of magnitude association with the rupture distances. For instance, the new method estimates durations of 2.0 s (Table 4) for the 20-km rupture distance, but the largest event in Table 1 does not contribute to this duration estimate, because the accelerogram with the shortest rupture distance of this event is 51.3 km (Table 3). The duration estimates proposed are based on a quite limited dataset, because suitable records are few. The Fennoscandian bedrock is classified as very-hard ($V_{s30} > 3000$ m/s), which implies that accelerograms from stations on softer rocks are in contradiction with prevailing local site conditions. This has also been an issue for the GMPE development, when a relatively small number of recordings were used (Fülöp et al. 2020). All events used for the duration estimates were recorded on very-hard rock (VHR) and excluded site-specific features, such as soil amplification. If a seismic event were recorded on soil, the method would still capture the strongest parts of the accelerogram. However, this should be tested with datasets other than VHR recordings.

The piecewise-linear regression fitting to the deviation curves of I_A is the core of the new method, and some of the main features require closer scrutiny. An important feature is the efficiency of calculating the deviation curves, which are dependent primarily on the time step Δt chosen in Fig. 1. Calculation of the deviation curve for 71 events with time steps 0.5 s and 1.0 s requires several minutes with an efficient laptop. The chosen time step Δt not only affects the calculation time, but also down-samples the original sampling frequency of the ground-motion data. Down-sampling smoothens the deviation curve for which the piecewise linear regression is easier to fit. This fitting by Muggeo (2003) and implemented to Python by Pilgrim (2021) is a powerful method for estimating the location of break-points on time axes, but it can be numerically challenging if the ground motions are recorded close to a ruptured fault and the accelerogram includes several cycles of large amplitudes. Despite this shortcoming, using the piecewise linear regression fitting in the estimation of ground-motion durations is promising. Fig. 6 reveals the importance of piecewise linear regression fitting. Body waves in the recordings from longer rupture distances are masked by the scattered waves, which makes it difficult to distinguish the beginning and end of the strongest motion in the accelerogram. This explains the spreading of the 95 % confidence intervals with longer durations. However, finding the beginning and the end of the linear range in the deviation curve becomes very subjective without using the piecewise linear regression fitting. In contrast, the linear range in the deviation curve is easy to determine when the 95 % confidence intervals are clustered. The analysis of duration residuals in Fig. 10 indicates that the piecewise linear regression fitting is reasonable since the duration residuals are quite evenly distributed around the mean. An exception appears at rupture distances further than 170 km, in which the residuals are close to the mean, due to the limited number of recordings. In conclusion, we propose to replace any method relying on fixed limits, such as 5 %–75 % accumulations of I_A , by the proposed method to define the durations of moderate earthquakes for structural analysis of NPPs.

Finally, we discuss the feasibility of using the proposed durations in floor vibration analysis of NPPs, utilization of the durations in floor vibration analysis of NPPs and compare the durations with the values given by the NRC (2020). The feasibility study demonstrates the similarities between all considered accelerograms in the Y and Z directions. Slight differences are present in the X direction. These differences in PSAs are not surprising because the duration in the X direction is not equal to the durations in the Y and Z direction. The Y direction at the St-Ferreol station had the largest Arias intensity, which defined duration in

that direction as the representative value (Table 3). Therefore, it is surprising that duration in the Y direction resulted in similar PSAs in the Z direction as the subplots (b) and (c) show in Figs. 13, 14, and 15. These subplots also show that the proposed duration is feasible and justified. The proposed method does not limit defining a single duration for each station. Instead of that, the duration could be defined for all three translational components of accelerogram. Two alternatives are available for utilizing the durations of Table 4 in floor vibration analysis of NPPs. The first option is a weighted scenario-based structural analysis, in which the duration is dependent on the rupture distances, as shown in Table 4. Thus, six durations in Table 4 are the parameters for the transformation of design response spectra to acceleration time histories. This process is computationally more demanding than the second option, which is the selection of rupture distance is dependent on the highest probability in the disaggregation of the seismic hazard. In Finland, the highest contribution to the seismic hazard is from the rupture distance range of 50–80 km. Interestingly, the mean duration of 6.1 s for 50 km in Table 4 is very close to the minimum duration of 6.0 s, which the NRC provisions (2020) give for the seismic design of NPPs. However, the 6.0-s duration by the NRC was not a conclusion of the analysis of the ground motions. Instead, the argument for the 6.0 s is to guarantee enough cycles for the Fast Fourier Transform. The mean duration of 7.0 s for the rupture distance of 80 km is reasonable, and fits in the duration range of 6.0–15.0 s by NRC (2020). The method to calculate duration in ASCE 4-16 (2017) is equivalent with the NRC method. The only difference is the constant $\pi/(2g)$ in front of the integral in Equation (5). The major difference between the durations in Table 4 and the durations by the NRC and ASCE is that neither of them provides durations as a function of distance. The authors are not aware of any public article in which durations are associated with distance defined from disaggregation of the seismic hazard. Similarly, as in the calculations of seismic hazard, the most critical factor in the assessment of the ground-motion durations is a sparse number of suitable events. The use of plausible synthetic ground motions may improve the situation.

7. Conclusions

This study introduces a new method to estimate the duration of ground acceleration for low seismicity regions. The duration is needed to transform design response spectra to time domain for floor vibration analysis of NPPs. The study confirms that a method commonly applied to estimate the ground-motion duration based on the 5 %–75 % accumulation of the Arias intensity (I_A) results in the durations that are unreasonable long of the ground accelerations for moderate earthquakes, since the accumulation of the I_A frequently extended to the nonlinear range.

The proposed method is based on accumulation of the I_A of an accelerogram. Calculating the I_A for a complete and repeatedly reduced time frames resulted in the I_A deviation curve. Interpretation of the beginning and end of the linear interval in the deviation curve can be subjective. A solution for avoiding subjective decisions was a piecewise linear regression fitting onto the deviation curve. The fitting included several break-points, and the time difference between the break-points closing in the steepest linear interval of the deviation curve defines the duration.

To apply the proposed method for the structural analysis of NPPs in Finland, a piecewise linear regression was fitted onto the rupture distance-dependent mean-duration point cloud. The fitting provided durations of 6.1 s and 7.3 s for 50 km and 100 km, respectively. The main advantage of the proposed method is that the durations are driven by features in ground-motion data. We propose applying this method to estimate the duration of moderate earthquakes for Fennoscandia, but the method should be applicable for earthquakes in other site conditions than those in this study. On the other hand, it seems that the duration is insensitive of moment magnitude (M_w) for short rupture distances. This indicates that smaller events can be useful for estimating duration

despite the events do not fulfill the requirements of design basis earthquake (DBE) or design extension earthquake (DEC) in terms of the peak ground acceleration (PGA). The feasibility study considered floor vibrations of a reactor building. The results show that the complete, reference and proposed accelerograms induce very similar floor acceleration in terms of pseudo-spectral acceleration (PSA) and cumulative distribution function (CDF) of peak floor accelerations. The calculated durations can be utilized in structural analysis of NPPs, either by applying the probability-weighted scenario-based structural analysis for various rupture distances, or by defining the duration for the rupture distance that has the largest seismic hazard.

CRedit authorship contribution statement

Vilho Jussila: Writing – original draft, Visualization, Validation, Software, Methodology, Investigation, Formal analysis, Data curation, Conceptualization. **Ludovic Fülöp:** Writing – review & editing, Supervision, Project administration, Funding acquisition. **Päivi Mäntyniemi:** Writing – review & editing. **Jari Puttonen:** Writing – review & editing, Supervision, Funding acquisition, Conceptualization.

Declaration of competing interest

The authors declare the following financial interests/personal relationships which may be considered as potential competing interests: This work is part of the project Sensitivity and risk informed seismic hazard updates (SERIOUS, Grant number: VN/21022/2022) that belongs to the SAFER2028 research programme (<https://safer2028.fi>) funded by the National Nuclear Waste Management Fund (VYR). Vilho Jussila reports financial support was provided by the Foundation for Aalto University Science and Technology, Finland. If there are other authors, they declare that they have no known competing financial interests or personal relationships that could have appeared to influence the work reported in this paper.

Data availability

Links to data are provide in paragraph Data availability. Some of studied events are available upon request.

Acknowledgments

Authors express gratitude for the National Nuclear Waste Management Fund (VYR) funding of the SERIOUS project (Grant number: VN/21022/2022) and the Foundation for Aalto University Science and Technology, Finland. The Radiation and Nuclear Safety Authority of Finland (STUK), is acknowledged for continuous support of seismic safety related research.

Natural Resources of Canada provided waveforms of 1988 Saguenay earthquake applied in this study upon request.

Doctor James Thompson (PhD) provided professional assistance in English during the preparation of this manuscript. He is not responsible for the final version of the manuscript.

References

- Abaqus, 2016. *ABAQUS/Standard User's Manual, Version 2017*. Dassault Systèmes Simulia Corp, United States.
- Abrahamson, N.A., Silva, W.J., 1997. Empirical response spectral attenuation relations for shallow crustal earthquakes. *Seismol. Res. Lett.* 68, 94–127. <https://doi.org/10.1785/gssrl.68.1.94>.
- Aki, K., Chouet, B., 1975. Origin of coda waves: source, attenuation, and scattering effect. *J. Geophys. Res.* 80, 3322–3342. <https://doi.org/10.1029/JB080i023p03322>.
- Ambraseys, N.N., Sarma, S.K., 1967. The Response of Earth Dams to Strong Earthquakes. *Géotechnique* 17, 181–213. <https://doi.org/10.1680/geot.1967.17.3.181>.
- Arias, A., 1970. A measure of earthquake intensity. In: Hansen, R. (Ed.), *Seismic Design for Nuclear Power Plants*. MIT Press, Cambridge, Massachusetts, pp. 438–483.
- ASCE 4-16, 2017. Seismic analysis of safety-related nuclear structures. <https://doi.org/10.1061/9780784413937>.
- ASCE 4-98, 2000. Seismic analysis of safety-related nuclear structures and commentary.
- Assatourians, K., Atkinson, G., 2010. Database of processed time series and response spectra data for Canada: an example application to study of 2005 MN 5.4 Riviere du Loup, Quebec, earthquake. *Seismol. Res. Lett.* 81, 1031. <https://doi.org/10.1785/gssrl.81.6.1013>.
- Bolt, B.A., 1973. Duration of strong ground motions, in: *Proceedings of Fifth World Conference on Earthquake Engineering*. Rome, Italy, pp. 1304–1313.
- Bommer, J.J., Martínez-Pereira, A., 1999. The effective duration of earthquake strong motion. *J. Earthq. Eng.* 3, 127–172. <https://doi.org/10.1080/13632469909350343>.
- Chandramohan, R., Baker, J.W., Deierlein, G.G., 2016. Quantifying the influence of ground motion duration on structural collapse capacity using spectrally equivalent records. *Earthq. Spectra* 32, 927–950. <https://doi.org/10.1193/1.22813eqs298mr2>.
- Dundulis, G., Kaciānauskas, R., Markauskas, D., Stupak, E., Stupak, S., Šliaupa, S., 2017. Reanalysis of the floor response spectra of the Ignalina nuclear power plant reactor building. *Nucl. Eng. Des.* 324, 260–268. <https://doi.org/10.1016/j.nucengdes.2017.09.009>.
- Fülöp, L., Jussila, V., Aapsuo, R., Vuorinen, T., Mäntyniemi, P., 2020. A ground-motion prediction equation for Fennoscandian nuclear installations. *Bull. Seismol. Soc. Am.* 110, 1211–1230. <https://doi.org/10.1785/0120190230>.
- Fülöp, L., Mäntyniemi, P., Malm, M., Toro, G., Crespo, M.J., Schmitt, T., Burck, S., Välikangas, P., 2023. Probabilistic seismic hazard analysis in low-seismicity regions: an investigation of sensitivity with a focus on Finland. *Nat. Hazards*. <https://doi.org/10.1007/s11069-022-05666-4>.
- Goulet, C.A., Bozorgnia, Y., Al Atik, L., Youngs, R.R., Graves, R.W., Atkinson, G.M., 2021. NGA-East ground-motion characterization model part I: summary of products and model development. *Earthq. Spectra* 37, 1231–1282. <https://doi.org/10.1177/87552930211018723>.
- Harris, C.R., Millman, K.J., van der Walt, S.J., et al., 2020. Array programming with NumPy. *Nature* 585, 357–362. <https://doi.org/10.1038/s41586-020-2649-2>.
- IAEA, 2021. Seismic design for nuclear installations (No. SSG-67), IAEA Safety Standards Series. Vienna.
- Jussila, V., Li, Y., Fülöp, L., 2016. Statistical analysis of the variation of floor vibrations in nuclear power plants subject to seismic loads. *Nucl. Eng. Des.* 309, 84–96. <https://doi.org/10.1016/j.nucengdes.2016.09.005>.
- Husid, R., 1969. Características de Terremotos. *Analisis General. Rev. Idiem* 8, 21–42.
- Kempton, J.J., Stewart, J.P., 2006. Prediction equations for significant duration of earthquake ground motions considering site and near-source effects. *Earthq. Spectra* 22, 985–1013. <https://doi.org/10.1193/1.2358175>.
- Kramer, S.L., 1996. *Geotechnical Earthquake Engineering, Prentice-Hall International Series In Civil Engineering And Engineering Mechanics*. Prentice Hall, Upper Saddle River, N.J.
- Ladak, S., Molner, S., Palmer, S., 2021. Multi-method site characterization to verify the hard rock (Site Class A) assumption at 25 seismograph stations across Eastern Canada. *Earthq. Spectra* 37, 1487–1515. <https://doi.org/10.1177/87552930211001076>.
- McGuire, R.K., 2008. Probabilistic seismic hazard analysis: Early history. *Earthq. Eng. Struct. Dyn.* 37, 329–338. <https://doi.org/10.1002/eqe.765>.
- Muggeo, V.M.R., 2003. Estimating regression models with unknown break-points. *Stat. Med.* 22, 3055–3071. <https://doi.org/10.1002/sim.1545>.
- Munro, P.S., North, R.G., 1988. Saguenay Earthquake of November 25, 1988 Strong Motion Data. Geological Survey of Canada Open File Report Number 1976, Ottawa.
- Natural Resources Canada, 1975. Canadian national seismograph network. <https://doi.org/10.7914/SN/CN>.
- NRC, 2020. Assessment of artificial acceleration time history guidance in standard review plan section 3.7.1 seismic design parameters (No. RIL 2019-01). United States Nuclear Regulatory Commission.
- Nuttli, O.W., 1973. Seismic wave attenuation and magnitude relations for eastern North America. *J. Geophys. Res.* 78, 876–885. <https://doi.org/10.1029/JB078i005p00876>.
- Page, R.A., Boore, D.M., Joyner, W.B., Coulter, H.W., 1972. Ground motion values for use in the seismic design of the Trans-Alaska pipeline system. *Geol. Survey Circul.* 672.
- Pilgrim, C., 2021. Piecewise-regression (aka segmented regression) in Python. *J. Open Source Softw.* 6, 3859. <https://doi.org/10.21105/joss.03859>.
- Sandberg, J., Välikangas, P., Varpasuo, P., 2008. The Finnish approach to seismic hazard analysis – case Loviisa. *ECD-NEA Workshop on Recent Findings and Developments in PSHA Methodologies and Applications*. Lyon, France.
- Somerville, P.G., MacLaren, J.P., Saikia, C.K., Helmberger, D.V., 1990. The 25 November 1988 Saguenay, Quebec, earthquake: source parameters and the attenuation of strong ground motion. *Bull. Seismol. Soc. Am.* 80, 1118–1143. <https://doi.org/10.1785/BSSA0800051118>.
- Sonley, E., Atkinson, G.M., 2005. Empirical Relationship between Moment Magnitude and Nuttli Magnitude for Small-magnitude Earthquakes in Southeastern Canada. *Seism. Res. Lett.* 76, 752–755. <https://doi.org/10.1785/gssrl.76.6.752>.
- STUK, 2019. Guide YVL B.7 Provisions for Internal and External Hazards at a Nuclear Facility.
- Tafampas, I.M., Spyarakos, C.C., Koutromanos, I.A., 2009. A new definition of strong motion duration and related parameters affecting the response of medium-long period structures. *Soil Dyn. Earthq. Eng.* 29, 752–763. <https://doi.org/10.1016/j.soildyn.2008.08.005>.
- Trifunac, M.D., Brady, A.G., 1975. A study on the duration of strong earthquake ground motion. *Bull. Seism. Soc. Am.* 65, 581–626. <https://doi.org/10.1785/BSSA0650030581>.
- Varpasuo, P., Nikkari, Y., van Gelder, P., 1999. Ground motion attenuation uncertainties for intraplate earthquakes with an application to southern Finland. *Safety and*

- Reliability: Proceedings of ESREL. Presented at the the Tenth European Conference on Safety and Reliability, Munich-Garching, Germany.
- Virtanen, P., Gommers, R., Oliphant, T.E., et al., 2020. SciPy 1.0: fundamental algorithms for scientific computing in Python. *Nat. Methods* 17, 261–272. <https://doi.org/10.1038/s41592-019-0686-2>.
- Weichert, D., 1985. New Brunswick strong ground motion records. *Phys. Earth Planet. Inter.* 38, 83–91. [https://doi.org/10.1016/0031-9201\(85\)90147-5](https://doi.org/10.1016/0031-9201(85)90147-5).
- Xie, L., Zhang, X., 1988. Engineering duration of strong motion and Its effects on seismic damage. In: *Proceedings of Ninth World Conference on Earthquake Engineering*. Tokyo-Kyoto, Japan, pp. 307–312.
- Zahrah, T.F., Hall, W.J., 1984. Earthquake energy absorption in SDOF structures. *J. Struct. Eng.* 110, 1757–1772. [https://doi.org/10.1061/\(ASCE\)0733-9445\(1984\)110:8\(1757\)](https://doi.org/10.1061/(ASCE)0733-9445(1984)110:8(1757)).